Relative ligand binding to small or large aggregates measured by scanning correlation spectroscopy

P. R. St-Pierre and N. O. Petersen
The Department of Chemistry, The University of Western Ontario, London, Ontario, Canada N6A 5B7

ABSTRACT Cell surface receptors transduce signals, required to produce cellular activity, that may be mediated by ligand-induced receptor aggregation. Several receptor systems exhibit both low and high ligand affinities and some models of receptor activation associate receptor clusters with high or low ligand binding affinity. In the present work succinyl concanavalin A, which binds with both high and low affinity to receptors, was studied on 3T3 Swiss mouse fibroblasts, where preaggregation of receptors has been postulated. Scanning fluorescence correlation spectroscopy measurements were used to determine the relationship between the degree of ligand binding and the state of receptor aggregation. Correlation analysis of fluorescence fluctuations across the cell surface reveal that the variance of the fluctuations (quantitated by g[0]) *increased* when the ligand concentration was varied from 0.33 to 67 mg/L. The $g(0)$ values reached a plateau at concentrations $>\sim 10$ mg/L. These data are incompatible with homogeneous receptor distributions or equal affinity receptor binding but are compatible with a partly aggregated receptor system with high affinity binding to small aggregates, and low affinity binding to large aggregates. Computer simulated scanning fluorescence correlation spectroscopy experiments confirm that background fluorescence from the cell does not account for the experimentally observed effects.

INTRODUCTION

Cell surface receptors provide one means by which the cell interacts with its surroundings. Activated receptors transduce signals required to produce cellular activity. The mechanism whereby this activation takes place is not fully understood. However, ligand-induced receptor aggregation appears to play an important role in some cases of transmembrane signaling (1–3). Schlessinger proposed a model in which the binding of ligands induces receptor clustering (4). The model implies that (*a*) monomers and receptor clusters are in equilibrium before ligand binding, (*b*) the ligand has preferential affinity to one of the receptor populations (monomers or clusters), and (*c*) the binding of ligand stabilizes the receptor population which possesses the enhanced enzymatic activity. This model has yet to be verified and raises questions about whether or not the receptors are partly aggregated at the cell surface before ligand binding.

Lectins have been very useful in studies of cell surface phenomena such as patching and capping, internalization, and receptor dynamics in general (5, 6). Although there are no real biological functions known for lectins on mammalian systems, they are attractive models because their activity is mediated by initial binding to saccharide-containing surface receptors and can be inhibited specifically with simple sugars. In most cases, a lectin binds to many distinct receptors, but frequently with comparable affinity because of its narrow sugar specificity. For example, concanavalin A binds primarily to D-glucose and D-mannose containing glycoproteins or glycolipids.

Receptor aggregation has also been studied using concanavalin A and other lectins as model systems. Aggregation was observed by fluorescence and electron microscopy (7–9) and was inferred from fluorescence energy transfer experiments (10, 11). Quantitative measurements of the extent of lectin aggregation on cultured cells have been difficult. Studies using electron microscopy in which one measures the radial size of particles have been attempted (12). Recently, Petersen introduced Scanning Fluorescence Correlation Spectroscopy (S-FCS) as a tool to measure the mean receptor aggregate size in cultured cells also employing lectins as models (13). The technique is based on a fluctuation analysis of the fluorescence intensity recorded when a focused laser beam is scanned across the surface of appropriately labeled cells. The concept of correlation fluctuation spectroscopy was initially proposed by Elson and Magde (14). More recently, higher order autocorrelation functions were introduced to characterize molecular aggregation (15, 16). The present work limits itself to first order autocorrelation functions.

The concepts of S-FCS have been presented elsewhere (13, 17). In summary, the amplitude of the photocurrent autocorrelation function is inversely proportional to the density of independently distributed fluorescent molecules at the cell surface. More explicitly, one can write

$$g(0) = \frac{1}{V}\sum_j (\epsilon_j Q_j)^2 \langle c_j \rangle \Big/ \Big(\sum_j \epsilon_j Q_j \langle c_j \rangle\Big)^2, \qquad (1)$$

0006-3495/90/08/503/09 $2.00

where ϵ_j represents the molar extinction coefficients, Q_j the quantum yields of fluorescence and $\langle c_j \rangle$ the average concentration of species j in the measurement volume, V. A receptor aggregate will contribute as a single independent species, even though it contains many subunits, because the positions of the monomers within an aggregate are interdependent and therefore correlated. The $g(0)$ value will depend on the different concentrations ($\langle c_j \rangle$) and sizes ($\epsilon_a Q_a = n\,\epsilon_m Q_m$, a:aggregates, m:monomers) of the aggregates present (monomers being a special case of a cluster with $n = 1$), and will represent the *receptor* distribution on the cell surface provided that every receptor is tagged with a fluorescent ligand, that is, they are saturated. Otherwise, $g(0)$ will reflect the *ligand* distribution on the receptors. Thus, $g(0)$ values from concentration-dependent experiments will represent changing ligand distributions on the fixed underlying receptor populations and will therefore give indirect information about the way that the receptors are distributed on the cell surface.

In this paper, we report on S-FCS experiments as a function of concentration of fluorescein-labeled and succinylated concanavalin A on 3T3 cells and show that these data reveal information about the receptor distributions and their relative affinities toward ligand binding. We use a Scatchard binding model to probe the effects of high and low binding affinities of ligands toward different receptor distributions on the experimental data. Computer simulations are performed to examine cell fluorescence background effects and to demonstrate the effects of small, high-affinity clusters.

MATERIALS AND METHODS

Materials

Fluorescein isothiocyanate succinyl concanavalin A (FITC-SconA) was purchased from Sigma Chemical Co. (St. Louis, MO). The SconA contains 1.6 mol of FITC per mole of protein. 3T3 Swiss Mouse Fibroblast and Dulbecco Modified Essential Medium (DMEM) supplemented with 10% calf serum and containing sodium pyruvate, streptomycin, and penicillin were both obtained from The Cancer Research Centre at The University of Western Ontario. Phosphate Buffered Saline solution (PBS) was prepared by diluting 10x concentrated PBS (Gibco Laboratories Life Technologies, Inc., Grand Island, NY). Trypsin 1:250 (Gibco Laboratories Life Technologies, Inc.) was dissolved in PBS to a final concentration of 1.5 mg/mL. Filtering of the solutions through a presterilized membrane filter, 0.20 μm pore size (Nalge Co., Rochester, NY), was required for sterilization. Paraformaldehyde (Fisher Scientific, Toronto, Canada) was dissolved in a basic aqueous solution (pH = 10) to a final concentration of 3% (wt/vol).

Cell culture and labeling

3T3 Fibroblasts were cultured in T25 flasks (Corning Glass Works, Corning, NY) with DMEM to subconfluency (10^6 cells per flask). After trypsinization the cells were diluted in 7.5 mL of medium, 0.2 mL of which was transferred to a 35-mm-diam tissue culture dish (Becton Dickinson Labware, Lincoln Park, NJ). The cells were allowed to grow for 48 h before labeling and S-FCS experiments. Cells were then washed three times with PBS, incubated at 37°C for 20 min with 3% paraformaldehyde solution for fixation. The cells were rewashed with PBS and incubated with a PBS solution of FITC-SconA at room temperature for 10 min. The final concentrations of FITC-SconA ranged from 0.3 to 67 mg/L. The cells were finally washed twice with PBS and mounted under the microscope objective for experiments.

S-FCS experiments

S-FCS measurements, the calculations of the photocurrent autocorrelation function and the fitting procedures were performed as described earlier (13). The cells were translated linearly over a range of 30 μm in 1,024 steps. The laser beam radius (W) of 1.10 ± 0.06 μm at the 40x objective focal point was measured with the gold edge method (18). The $g(0)$ values are reported as an average of N measurements each of which fit the criteria that the fitted beam radius W_f be within 30% of the measured value. The total number of measurements for each set of conditions are reported in Table 1. The standard error of the mean (SEM) was calculated using the student's t-test value with N-1 degrees of freedom and 95% level of confidence.

Computer simulations

All simulations were performed using Fortran vectorial source code on an ETA10 computer system at Computing and Communications Services, The University of Western Ontario. Receptor populations on the cell surface were simulated by generating randomly distributed points on a 40 × 10 μm imaginary surface at the nanometer resolution level. The random number generator used a multiplicative congruential method (19). The form of the generator was,

$$x_i \equiv c\,x_{i-1} \bmod (2^{31} - 1),$$

where the multiplier c was taken as 950706376. Each point (j) was assigned a proper intensity value (p_j). The simulated fluorescence intensity data record was calculated as follows:

$$F(k \cdot \Delta x) = \Sigma_j\, p_j(x, y) \cdot I(x, y) \cdot E(x, y),$$

where

$$I(x, y) = I_0 \exp -2\{[x - (x_0 + k\Delta x)]^2 + [y - y_0]^2\}/W^2$$

is the cross-sectional intensity distribution of the incident laser irradiation and

$$E(x, y) = \exp - \{[x - (x_0 + k\Delta x)]^2\}/S^2$$

is the transmission profile of the microscope pinhole aperture (S) in the image plane (20). The sum is over all points j within four beam radii (W) from the center of the laser beam ($x_0 + k\Delta x, y_0$). The variation along the z direction for these functions (20) was not included because the surface was considered to be flat and at the focal plane. The scanning step size is represented by Δx and k is an integer that ranges from 0 to 1,024, the full scanning distance being ~30 μm. The autocorrelation function, the $g(0)$, and SEM values were determined as described above.

RESULTS AND DISCUSSION

To test whether S-FCS can discriminate between the high and low affinity components of certain receptor systems, we performed S-FCS experiments of SconA as a function of concentration on 3T3 Swiss mouse fibroblasts. The motivation for using the concanavalin A receptor system is that the concanavalin A receptors are known to possess both high and low affinity sites on human fibroblasts (21). Binding studies with radiolabeled concanavalin A reported Scatchard plots with two distinct lines corresponding to binding constants on the order of 10^{+9} and 10^{+6} M^{-1} for the high and low binding sites. Our objective was to assign concanavalin A binding affinity sites to specific receptor populations.

Table 1 summarizes concentration dependent S-FCS measurements of SconA ligand distributions on 3T3 cells. The $g(0)$ values are plotted in Fig. 1 as a function of the FITC-SconA concentration presented to the cells. The first data point with no SconA added is a measurement of the background fluorescence on unlabeled cells. As the concentration increases to 10 mg/L, the $g(0)$ values increase to reach a plateau of ~0.1. The plateau is observed over a range from 10 to 67 mg/L of FITC-SconA. No values were measured above 67 mg/L. Small values of $g(0)$ indicate a large number of independent particles and, correspondingly, large values of $g(0)$ indicate a small number of independent particles in the measurement volume. Thus, as the concentration of FTIC-SconA increases, more and more ligand binds to the cell receptors, but it appears that a smaller number of independent particles per measurement volume is observed. This is counterintuitive for homogeneous receptor populations. Rather, the experimental observations suggest a heterogeneity in receptor distribution, a difference in receptor binding affinities, or a combination of both factors.

TABLE 1 Experimental and fitting parameters for the S-FCS experiments

[FITC-SconA]	$g(0)$	SEM	$\langle i \rangle$	# Cells*
L/mg				
0	0.003	0.001	32	11/15
0.333	0.011	0.009	78	10/20
1.33	0.030	0.014	395	7/16
3.333	0.071	0.030	662	7/10
16.7	0.112	0.027	2530	8/13
33.3	0.114	0.023	1416	9/10
41.7	0.103	0.014	2480	36/38
66.7	0.120	0.021	5370	10/10

*The numbers to the right of the slash indicate the number of cells subjected to S-FCS experiments, the numbers to the left indicate that which fit the criteria of selection (Materials and Methods).

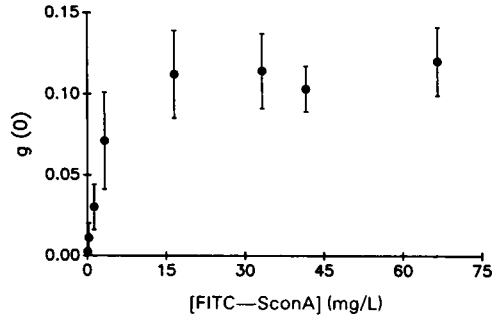

FIGURE 1 Zero time values of the photocurrent autocorrelation function $g(0)$ measured on 3T3 Swiss Mouse Fibroblasts as a function of FITC-Scon A concentration in solution. The error bars represent SEM values calculated with 95% level of confidence.

To explore these possibilities, we analyze the concentration dependence of $g(0)$ for mixed populations of monomeric and aggregated receptors with different affinities for ligand binding. The $g(0)$ values are calculated according to Eq. 1 with a Scatchard ligand binding model used to obtain the ligand distributions (c_j).

Mixed receptor populations with equal ligand affinity

The dependence of $g(0)$ on ligand concentration is examined for two distinct receptor distributions at the cell surface, (*a*) monodispersed and (*b*) clustered. The ligand distribution on the receptor population for a specific ligand concentration $[L]$ is given by the association equilibrium equation for the monomers and a Scatchard analysis for the aggregates.

(*a*) For the monomer population, the equilibrium equation is given by

$$R_m + L \underset{K_m}{=} R_m L \tag{2}$$

yielding the labeled monomer concentration $[R_m L]$:

$$[R_m L] = [R_m]\, K_m\, [L], \tag{3}$$

where $[R_m]$ is given by the total concentration of monomers in a given measurement volume, $[R_m T]$, minus the concentration of receptor that is occupied by a ligand, $[R_m L]$. In terms of $[R_m L]$, Eq. 1 simply becomes (13)

$$g(0) = \frac{1}{V} \cdot \frac{1}{[R_m L]}. \tag{4}$$

(*b*) For the aggregate population, the series of equilibria are

$$\begin{aligned} R_a + L &\underset{K_a}{=} R_aL \\ R_aL + L &\underset{K_a}{=} R_aL_2 \\ &\vdots \\ R_aL_{j-1} + L &\underset{K_a}{=} R_aL_j \\ &\vdots \\ R_aL_{N-1} + L &\underset{K_a}{=} R_aL_N. \end{aligned} \tag{5}$$

With the usual assumptions of equivalence and independence, i.e., that the binding is equal for all subunits and remains unchanged upon binding of a ligand, the Scatchard derivation yields the distribution of ligand on the aggregates with N binding sites

$$[R_aL_j] = \binom{N}{j} [R_a](K_a[L])^j, \tag{6}$$

where $[R_a] = [R_aT]/\Sigma_{j=0}^{N} \binom{N}{j} (K_a[L])^j$, $[R_aT]$ represents the total concentration of the aggregates in the measurement volume and $\binom{N}{j}$ is the binomial factor. This analysis excludes cross-linking effects from multivalent ligands. Eq. 1 leads to (13)

$$g(0) = \frac{1}{V} \cdot \frac{\Sigma_j j^2 [R_aL_j]}{(\Sigma_j j[R_aL_j])^2}. \tag{7}$$

One application of these equations is shown in Fig. 2 under conditions where the total number of independent particles is kept constant whereas the number of receptors per particle is varied. The objective of these calculations is to determine whether a concentration depencence of $g(0)$ is sensitive to the size of the aggregated particles. For illustrative purposes, the average number of particles (monomers, R_mT or aggregates, R_aT) were set at 30 per measurement volume. The number of monomers per aggregate (N) and the affinity constants, *Km* and *Ka*, used in the calculations are listed in Table 2. The results are presented in Fig. 2 *A* for the high affinity data and in Fig. 2 *B* for the low affinity data as a function of the total ligand concentration (in both cases this is the same as the free ligand concentration because <1% of the ligand added is bound to the receptors). The concentration unit assumes a molecular weight for the ligand of 56 kdal, the molecular weight of SconA. Comparison of Fig. 2, *A* and *B*, demonstrates the difference in concentration range

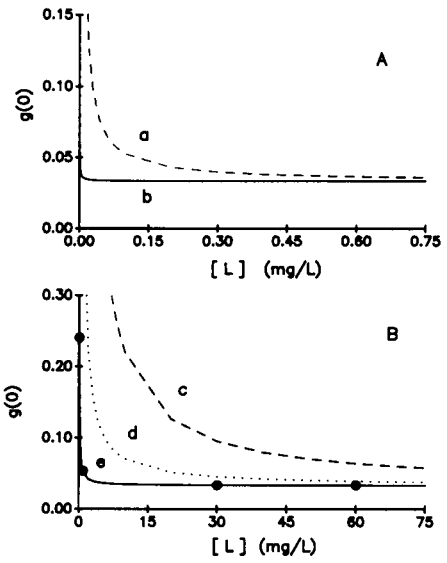

FIGURE 2 Calculated $g(0)$ values as a function of ligand concentration for two binding constants (*A*) 10^{+9} M^{-1} and (*B*) 10^{+6} M^{-1}. Curves *a* and *c* are calculated for a monodispersed receptor distribution of 30 monomers per measurement volume, whereas curves *b* and *e* are for an aggregated receptor distribution of 30 aggregates each with 100 receptors and curve *d* is for 30 aggregates each with only 5 receptors. A corresponding calculation of the variation in $g(0)$ with ligand concentration for a mixed receptor distribution of 30 monomers and 30 aggregates each with 100 receptors is indistinguishable from curve *e*. The solid circles indicate the combinations of concentrations and $g(0)$ values which correspond to the distributions shown in Fig. 3.

required to observe variations in $g(0)$ as the affinity constant changes.

It is evident for both high and low affinity constants that the $g(0)$ decreases more gradually for monomers than for an aggregated system. In fact, a highly aggregated system shows no concentration dependence except at extremely low concentrations. This was the basis for earlier conclusions (13) that conA receptors are at least partly aggregated before addition of ligands. These calculations, specifically the shape of the curves in Fig. 2, suggest that neither of these receptor distributions alone could correspond with the observed SconA receptor distri-

TABLE 2 Input parameters for calculations of *g* (0) for different aggregation states (Fig. 2)

	N	*Ka*	*Km*
a	1		10^{+9}
b	100	10^{+9}	
c	1		10^{+6}
d	5	10^{+6}	
e	100	10^{+6}	

bution on 3T3 fibroblasts particularly at low concentrations. Nevertheless, the asymptotic value of $g(0)$ will provide an estimate of the average number of independent particles, which can be classed as aggregates if the $g(0)$ is constant for an extended concentration range. Accordingly, the constant value of $g(0)$ in Fig. 1 at concentrations of FITC-SconA above 10 mg/L suggests a constant number of receptor aggregates being populated by the fluorescent lectin. The $g(0)$ value of 0.11 provides an estimate of nine aggregates per measurement volume because $g(0) = 1/N$.

A receptor distribution with a mixture of the two receptor populations predicts

$$g(0) = \frac{1}{V} \cdot \frac{[R_m L] + \Sigma_j j^2 [R_a L_j]}{([R_m L] + \Sigma_j j [R_a L_j])^2}. \quad (8)$$

The dependence of $g(0)$ on ligand concentration for the mixed receptor distribution where the two populations, monomers and aggregates, are being labeled with equal ligand affinity ($Km = Ka = 10^{+6}$ M^{-1}) coincides with curve *e* in Fig. 2. To understand this behavior, it is instructive to calculate the fraction of *ligand* bound to each of the two *receptor* populations at any free ligand concentration. This is illustrated in Fig. 3 for the four ligand concentration marked in Fig. 2 *B* by a solid circle. As the free ligand concentration is raised from 0.09 to 30 mg/L the fraction of ligand bound to the monomer population decreases to 0.01 corresponding to the total monomer fraction of 1% of the total receptor. Concommitantly, all the receptor aggregates become labeled with at least one ligand. As the concentration is increased further the number of aggregates that are being labeled remains constant, but the average number of ligand molecules per aggregate increases as seen by comparing Fig. 3, *C* and *D*.

At low concentration, $g(0)$ is high corresponding to a few receptors in monomers or aggregates detected per measurement volume. At high concentration, the aggregates dominate the contribution to the $g(0)$ value so that it reaches a plateau indicating a fixed number of aggregates. Thus, even the mixed receptor distribution with equal ligand binding affinities does not account for the SconA receptor distribution on 3T3 fibroblasts. The transition curve between the high and low concentration region does not agree with that observed experimentally. This transition is determined by the magnitude of the $[R_m L]$ terms in Eq. 8. Comparing the effect of affinity constant (Fig. 2, *A* and *B*) suggests that the shape of the curves will depend on the relative values of the equilibrium constants, *Km* and *Ka and* on the relative amount of single receptors in the monomer and aggregate forms.

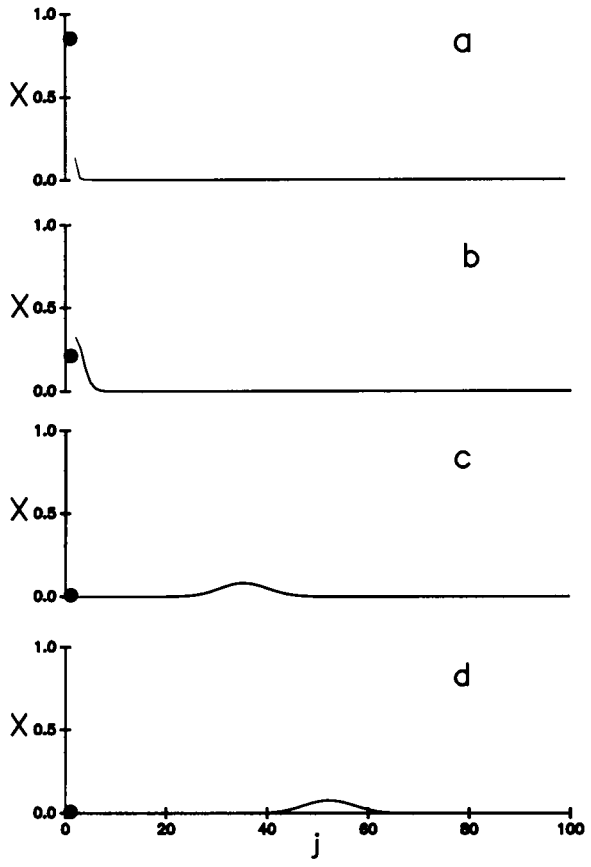

FIGURE 3 Calculated fractions of ligand bound to each of the two receptor populations, 30 monomers and 30 aggregates each with 100 receptors, for the following concentrations (*a*) 0.09 mg/L, (*b*) 0.9 mg/L, (*c*) 30 mg/L, (*d*) 60 mg/L (see Fig. 2). The solid circles correspond to the fraction of ligand bound to the monomer population and the continuous lines represent the distribution of ligand bound to the aggregates.

Mixed receptor populations with different ligand affinities

The equilibrium constants ratio, *Km/Ka,* establishes the relative affinity of the ligand for the different receptor populations. High values of Km/Ka indicate that the ligand has preferrential affinity to the monomers, making the $[R_m L]$ terms dominant over the $[R_a L_j]$ terms (Eq. 8). Correspondingly, low values of Km/Ka indicate that the aggregate population is primarily labeled with ligand, and the $[R_a L_j]$ terms dominate the $[R_m L]$ terms.

To examine the effect of the ligand affinity ratio, *Km/Ka,* on the shape of the curve of $g(0)$ as a function of ligand concentration, we have calculated $g(0)$ values according to Eq. 8 for identical receptor distributions, with three different Km/Ka ratios, 10^{-3}, 1, and 10^{+3}. The receptor distribution is composed of two receptor popula-

tions : monomers with $R_mT = 30$ and aggregates with $R_aT = 9$ and containing 100 monomers each capable of binding one ligand. The results of the calculations are compared in Fig. 4.

At high ligand concentration, when the receptor populations are saturated, the $g(0)$ values converge to the same value because they represent the true receptor distributions at the cell surface which are the same for the three cases. The $g(0)$ value of the plateau yields an average number of aggregates of 9.6, which agrees well with the theoretical input value for the calculation of 9.

The key differences between these curves are at low concentrations of ligand. For $Km/Ka = 10^{-3}$ the ligand binds to the aggregates preferentially. At low concentrations of ligand the population of aggregates dominates the contribution to the $g(0)$ values, resulting in a very rapid approach to the asymptotic value of $g(0)$ (*curve 4 a*). This corresponds to the aggregates dominating, as in Fig. 2, *b* and *e*. For equal ligand binding affinity, i.e., $Km/Ka = 1$ (*curve 4 b*), the shape of the curve is similar to that in curve 4 *a*. The additional binding of ligand to the monomer population has a small effect as noted in the context of Fig. 3. For $Km/Ka = 10^{+3}$ the ligand binds to the monomer population preferentially. At low concentrations of ligand the monomer population dominates the contribution to the $g(0)$ values, making the $1/[R_mL]$ behavior prominent (*curve 4 c*). The $g(0)$ value decreases to reach a minimum value of 0.033 corresponding to the larger population in the distribution (30 monomers compared with 9 aggregates per measurement volume). Once the monomer population gets saturated the aggregates become populated by the ligand and contribute to the $g(0)$ values. An increase in the $g(0)$ value with ligand concentration is then observed because the further labeling of the aggregates cause them to become brighter relative to the monomer population, so the monomers contribute progressively less to the $g(0)$ values.

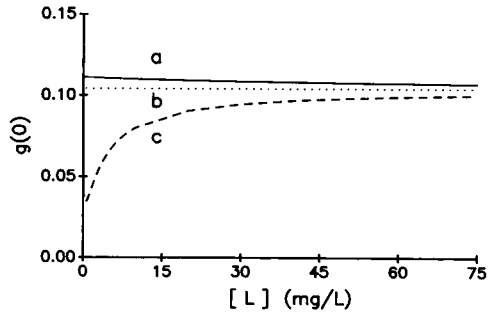

FIGURE 4 Calculated $g(0)$ values as a function of ligand concentration for three different affinity ratios (Km/Ka), (*a*) 10^{-3}, (*b*) 1, (*c*) 10^{+3} (see text).

The experimental results of Fig. 1 resemble curve 4 *c* with the exception that at very low ligand concentration large values of $g(0)$ are not seen. The shape of the curve and the smaller $g(0)$ values at concentrations below 10 mg/L of FITC-SconA suggest firstly that at least two populations of fluorescent species are present at the cell surface of 3T3 fibroblasts, and secondly that the population with a greater number of independent particles per measurement volume has higher affinity for the lectin and consists of small aggregates or monomers, whereas the population with a smaller number of independent particles has lower affinity for the lectin and consists of large aggregates of receptors.

Background fluorescence effect on $g(0)$

At low concentrations of ligand, the cell background fluorescence will contribute to the intensity and give rise to a smaller $g(0)$ value. The question is by how much? In cases where background fluorescence is Poisson distributed, the autocorrelation function obtained can be corrected (22, 23). However, cells present a nonuniform background fluorescence at their surface which makes correction impractical.

From Eq. 1, one can develop an expression that accounts explicitly for the species producing background fluorescence intensity:

$$g(0) = \frac{1}{V}\frac{(\epsilon_1 Q_1)^{-2}\Sigma_b(\epsilon_b Q_b)^2\langle c_b\rangle + \langle R_mL\rangle + \Sigma_{j=1} j^2\langle R_aL_j\rangle}{((\epsilon_1 Q_1)^{-1}\Sigma_b(\epsilon_b Q_b)\langle c_b\rangle + \langle R_mL\rangle + \Sigma_{j=1} j\langle R_aL_j\rangle)^2}. \quad (9)$$

Here the index 1 assigns spectroscopic caracteristics to the ligand and b to the background species. Eq. 9 assumes that fluctuations arising from the background species are not correlated with those arising from the ligand bound to its receptor. The presence of the background term in Eq. 9 can perturb the normal dependence of $g(0)$ on concentration as studied in the context of Fig. 2 and Fig. 4. In fact, one can obtain a curve similar to curve 4 *c* by replacing the high affinity monomer population with a fixed background fluorescence contribution. The extent of the perturbation will be determined by the amplitude of the background term. This term is governed by the contrast ratio $\epsilon_1 Q_1/\epsilon_b Q_b$. In cell work, background fluorescence can be substantial. Therefore, the brighter the ligand used, the less significant the background fluorescence becomes, and the lower the concentration that one can work with. The relative significance of the background fluorescence is illustrated in the experimental work presented below.

S-FCS experiments on simulated cell surfaces

Computer simulated S-FCS experiments were performed to determine whether cell background fluorescence or small oligomers of receptors contribute more to the $g(0)$ values at low concentration of FITC-SconA. The results of these simulations and their comparison with the real experimental results are shown in Fig. 5, where the total ligand concentration axis in Fig. 1 has been converted to the experimentally determined average fluorescence intensity ($\langle i \rangle$).

To link computer simulation with experimental results, it is necessary to assign the FITC-SconA concentration limits of the experiments to specific ligand distributions. The limits employed are (*a*) no FITC-SconA added to the cells corresponding to the contribution of cell background fluorescence alone to the $g(0)$ value, and (*b*) concentrations of FITC-SconA >10 mg/L, where the plateau is found, assuming that only the aggregate population contributes significantly to the $g(0)$ values. In each limit it is now possible to introduce a single point-population into the simulation with intensity distribution and number density chosen such that the $g(0)$ and average fluorescence intensity values from the simulated S-FCS experiment match those obtained in the cell experiments. The two point-populations obtained this way are then added for simulation of intermediate points. The high and low intensity limits obtained with the mixed point-population are indicated by the squares in Fig. 5. A decrease in concentration of FITC-SconA presented to the cells is simulated by a decrease in the assigned intensity value (p_j) to the aggregate point-population corresponding to fewer ligands bound per aggregate. Curve 5 *a* then represents the variation in $g(0)$ for a cell surface with only two fluorescent species, background and aggregates. It is clear that this particular receptor distribution does not adequately match the experimental results. The $g(0)$ values change from small to large values in a range of average fluorescence intensity which is too low, indicating that a third point-population should be introduced to produce the experimentally observed effect.

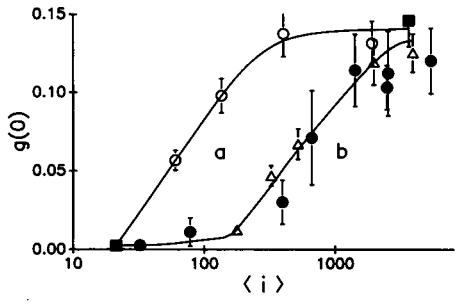

FIGURE 5 Comparison of experimentally determined $g(0)$ values with those obtained by computer simulations. The 3T3 cell data (●) are obtained from Table 1. The solid squares (■) represent simulation values obtained from the two limiting point-populations with cell background fluorescence only and aggregates only. The open circles (○ correspond to the $g(0)$ values from simulations with the point-populations representing both cell background and aggregates. For each point the intensity of the aggregates is varied in the simulation. The triangles (△) represent simulations in which a third point-population corresponding to high-affinity oligomers is added. Again, only the intensity of the aggregates is varied. These specific point-populations are described in Table 3. The lines shown are there solely as a visual aid and are not fit to the data.

Curve 5 *b* represents the variation in $g(0)$ obtained from simulations for a cell surface with three fluorescent species, background, oligomers (or monomers) and aggregates. The densities and assigned intensity values (p_j) of the three point-populations are given in Table 3. The simulation is achieved by decreasing the assigned intensity value (p_j) *of the aggregates only,* therefore assuming high ligand affinity for the oligomer population as suggested by Fig. 4 *c*. This particular receptor distribution resulted from a number of simulations successively refined to produce simulated values in good agreement with the experimental results. As the intensity decreases, the $g(0)$ value drops in about the same fashion as the experimental values, all the way back to the cell background fluorescence data point.

One could extract details of the oligomer population at the cell surface from actual curve fitting. This is difficult because the simulated values require extensive computing, are subject to random errors arising from the random assignment of the surface distribution and the fit must be to two variables: density, which is the number of oligomers per measurement volume, and intensity, which is the size of the oligomer. One must know the ratio $n\,\epsilon_1 Q_1/\epsilon_b Q_b$, where n is an integer representing the number of subunits per oligomer, to predict the density of the oligomer population. The n value can be obtained from the graph of $g(0)$ vs. ligand concentration only if the contrast ratio, $\epsilon_1 Q_1/\epsilon_b Q_b$, is large. At this point we cannot make that presumption.

In the case of the SconA receptor system, the oligomer

TABLE 3 Parameters used in the simulation of the S-FCS results presented in Table 1

	Density*	p_j
Background	45,000	1
Oligomers	10,000	25
aggregates	800	10,000

*The density is expressed per 400 μm^2. The total receptor density corresponds to $\sim 10^{+6}$ receptors per cell.

population is likely to be a different receptor type than that which constitute the aggregates because concanavalin A binds to a variety of glycoproteins and glycolipids at the cell surface. Nevertheless, S-FCS experiments as a function of ligand concentration are able to distinguish high and low affinity binding sites. For the SconA receptor system on 3T3 fibroblast, oligomers appear to possess the high affinity sites and the larger aggregates the low affinity sites for SconA binding.

CONCLUSION

The use of fluorescence correlation spectroscopy to determine the state of aggregation has been demonstrated in a few systems. The adaptation of a scanning technique extends the approach to cell surface receptor aggregation. The present work demonstrates that measurements as a function of ligand concentration will permit an estimate of the extent of aggregation as long as the binding constants are known. This is illustrated in Fig. 2 by the difference in concentration needed, depending on the binding constant, to affect a certain change in the $g(0)$ values. Of more general interest and potential use is the demonstration that the correlation analysis may be used to establish whether there are different binding affinities toward monomeric or aggregated receptors. When a ligand is known to bind with both high and low affinity to a cell surface, as in the case of concanavalin A, then we predict that the $g(0)$ values will *decrease* asymptotically if the aggregated receptors have higher affinity, *or* will *increase* asymptotically (at least over some concentration range) if the monomers have the higher affinity. In the specific case studied here, the latter is true. In cases where there is no independent evidence for more than one binding affinity, it is only if the monomeric species have the higher affinity that the S-FCS experiments provide new insight. This is because these experiments do not discriminate well between the binding only to aggregates and the binding to aggregates with high affinity. To observe these affinity effects the total concentration of ligand must be varied. If labeled ligand were diluted with unlabeled ligand at a constant total concentration, thereby keeping the surface binding unchanged, then the high affinity sites will be saturated with unlabeled ligand at high dilutions. They will not be detected at concentrations where their influence is most pronounced.

This work was supported by Natural Sciences and Engineering Research Council, Canada operating grant number 3272.

Received for publication 12 December 1989 and in final form 30 March 1990.

REFERENCES

1. Jacobs, S., and P. Cuatrecasas. 1985. The mobile receptor hypothesis and polypeptide hormone action. *Recept. Ligands Intercell. Commun.* 4:39–60.
2. Menon, A. K., D. Holowka, B. Baird, and W. W. Webb. 1986. Clustering, mobility, and triggering activity of small oligomers of immunoglobulin E on rat basophilic leukemia cells. *J. Cell Biol.* 102:534–540.
3. Schlessinger, J. 1986. Regulation of cellgrowth by the EGF receptor. *In* Oncogenes and Growth Control. P. Kahn and T. Graf, editors. Springer-Verlag Berlin, Heidelberg. 77–84.
4. Schlessinger, J. 1988. Signal transduction by allosteric receptor oligomerization. *TIBS (Trends Biochem. Sci.)* 13:443–447.
5. Singer, S. J., J. F. Ash, L. Y. W. Bourguigon, M. H. Heggeness, and D. Louvard. 1978. Transmembrane interactions and the mechanisms of transport of proteins across membranes. *J. Supramol. Struct.* 9:373–389.
6. Smith, B. A., W. R. Clark, and H. M. McConnell. 1979. Anisotropic molecular motion on cell surfaces. *Proc. Natl. Acad. Sci. USA.* 76:5641–5644.
7. Ash, J. F., and S. J. Singer. 1976. Concanavalin-A-induced transmembrane linkage of concanavalin A surface receptors to intracellular myosin-containing filaments. *Proc. Natl. Acad. Sci. USA.* 73:4575–4579.
8. Shotton, D., K. Thompson, L. Wofsy, and D. Branton. 1978. Appearance and distribution of surface proteins of the human erythrocyte membrane. An electron microscope and immunochemical labeling study. *J. Cell Biol.* 76:512–531.
9. Roos, D. S., J. M. Robinson, and R. L. Davinson. 1983. Cell fusion and intramembranous particle distribution in polyethylene glycol resistant cells. *J. Cell Biol.* 97:909–918.
10. Schreiber, A. B., J. Hoebke, B. Vray, and A. D. Strosberg. 1980. Evidence for reversible microclustering of lentil lectin membrane receptors on HeLa cells. FEBS (*Fed. Eur. Biochem. Sci.*) Lett. 111:303–306.
11. Dale, R. E., J. Novros, S. Roth, M. Edidin, and L. Brand. 1981. Application of Forster long-range excitation energy transfer to the determination of distributions of fluorescently-labelled concanavalin A-receptor complexes at the surfaces of yeast and normal and malignant fibroblasts. *In* Fluorescent Probes. G. S. Beddard and M. A. West, editors. Academic Press Inc., New York. 159–181.
12. Barber, K. R., I. E. Mehlhorn, and C. W. M. Grant. 1987. Double label freeze-etch study of the relative topography of concanavalin A and wheat germ agglutinin receptors at the myoblast surface. *Biochem. Biophys. Acta.* 902:395–401.
13. Peterson, N. O. 1986. Scanning fluorescence correlation spectroscopy, 1. Theory and simulation of aggregation measurements. *Biophys. J.* 49:809–815.
14. Elson, E. L., and D. Magde. 1974. Fluorescence correlation spectroscopy. 1. Conceptual basis and theory. *Biopolymers.* 13:1–27.
15. Palmer III, A. G., and N. L. Thompson. 1987. Molecular aggregation characterized by high order autocorrelation in fluorescence correlation spectroscopy. *Biophys. J.* 52:257–270.
16. Palmer III, A. G., and N. L. Thompson. 1989. High-order fluores-

cence fluctuation analysis of model protein clusters. *Proc. Natl. Acad. Sci. USA.* 86:6148–6152.

17. Madge, D., W. W. Webb, and E. L. Elson. 1978. Fluorescence correlation spectroscopy. III. Uniform translation and laminar flow. *Biopolymers.* 17:361–376.
18. Webb, W. W., and M. B. Schneider. 1981. Measurement of submicron laser beam radii. *Appl. Optics.* 20:1382–1388.
19. Lewis, P. A. W., A. S. Goodman, and J. M. Miller. 1969. A pseudo-random number generator for the system/360. *IBM Syst. J.* 2:136–146.
20. Koppel, D. E., D. Axelrod, J. Schlessinger, E. L. Elson, and W. W. Webb. 1976. Dynamics of fluorescence marker concentration as a probe of mobility. *Biophys. J.* 16:1315–1329.
21. Feller, M., C. Richardson, W. D. Behnke, and E. Gruenstein. 1977. High and low binding sites for concanavalin A on normal human fibroblasts *In Vitro. Biochem. Biophys. Res. Commun.* 76:1027–1035.
22. Koppel, D. E. 1974. Statistical accuracy in fluorescence correlation spectroscopy. *Physical Review A.* 10:1938–1945.
23. Thompson, N. L., and A. G. Palmer III. 1989. Intensity dependence of high-order autocorrelation functions in fluorescence correlation spectroscopy. *Rev. Sci. Instrum.* 60:624–633.